

Computational Studies of Chemical Shifts Using Density Functional Optimized Geometries. II. Isotropic ^1H and ^{13}C Chemical Shifts and Substituent Effects on ^{13}C Shieldings in 2-Adamantanone

Dražen Vikić-Topić^{a,*} and Ljupčo Pejov^b

^aRugjer Bošković Institute, NMR Center, P. O. Box 180, HR-10002 Zagreb, Croatia

^bInstitute of Chemistry, Faculty of Natural Sciences and Mathematics,
Cyril and Methodius University, P. O. Box 162, 91001 Skopje, Macedonia

Received December 15, 2000; revised February 19, 2001; accepted February 20, 2001

The ^1H and ^{13}C isotropic chemical shifts and the substituent effects thereof (with respect to adamantane), computed at the HF, BLYP, B3LYP/6-311G(d,p) as well as at MPW1PW91/6-311+G(2d,p) levels of theory with CSGT, GIAO and IGAIM algorithms, for the BLYP/6-31G(d,p) and B3LYP/6-31G(d,p) optimized geometries of 2-adamantanone are reported and compared with the experimental data. When absolute values of isotropic chemical shifts (with respect to TMS) are in question, the MPW1PW91/6-311+G(2d,p) level leads to excellent agreement with the experiment, while the HF approach is superior to the BLYP and B3LYP ones. However, the substituent effects on ^{13}C shieldings are better reproduced at the BLYP and B3LYP levels than at the HF level, while the MPW1PW91 approach is again significantly superior to all the others, leading to excellent agreement with experimental data. The most probable reason for these findings may be the cancellation of errors arising from the inappropriate description of the paramagnetic contributions to the overall shielding tensor within the Kohn-Sham approach, and the more systematic nature of errors in DFT approaches. The isotropic chemical shift values at all levels of theory, however, correlate excellently with the experimental data, the correlation being superior for DFT to the HF level of theory.

Key words: magnetic shielding, ^1H and ^{13}C isotropic chemical shifts, *ab initio* calculations, density functional theory, 2-adamantanone.

* Author to whom correspondence should be addressed. (E-mail: viki@faust.irb.hr)

INTRODUCTION

It is almost impossible to overestimate the significance of accurate prediction of various molecular response properties to external fields in almost all areas of chemical physics. The foregoing statement especially holds for second-order magnetic response properties. This is so because the magnetic resonance based techniques have become of substantial importance in chemistry and biochemistry. Let us briefly recall the general importance of these methodologies. The computed ^{13}C chemical shifts are frequently used as a valuable tool in identification of reactive ionic species,^{1–3} while the prediction of environmental dependence of the chemical shifts in the case of amino acid carbon atoms might be very helpful in elucidation of three-dimensional protein structures.^{4–7} Accurate prediction of chemical shifts may also be of invaluable help for determining the structures of molecules in solutions.

The nuclear magnetic shielding tensors, defined as the mixed second derivatives of energy (E) with respect to the magnetic moment of the X-th nucleus (\vec{m}_X) and the external magnetic field (\vec{B}), represented by the equation below⁸ (Greek superscripts denote the corresponding vector or tensor components):

$$\sigma_X^{\alpha\beta} = \frac{\partial^2 E}{\partial B^\alpha \partial m_X^\beta} \quad (1)$$

are of primary importance. However, it has been well recognized that a calculation of the second-order magnetic response properties from the first principles, using a finite basis set, requires a gauge-independent algorithm.^{10–14} A number of computational techniques have been proposed to achieve the gauge-invariance. We have discussed these algorithms in more detail in our previous paper,¹⁵ so only a brief overview will be given here. Within the so-called GIAO methodology (Gauge Independent Atomic Orbitals), based on the works of London and Ditchfield,^{8,9} the gauge-invariance is achieved using explicitly field-dependent basis functions.^{8–14} Application of the GIAO approach to molecular systems was significantly improved by an efficient implementation of the method for the *ab initio* SCF calculations, using techniques borrowed from analytic derivative methodologies.^{13,14} The second widely applied technique is the CSGT (Continuous Set of Gauge Transformations) algorithm^{9,16–18} due to Keith and Bader (and its variant known under the acronym IGAIM – Individual Gauge for Atoms In Molecules).^{16–18} In the CSGT approach, the nuclear magnetic shielding tensor is expressed through the induced first-order electronic current density. An accurate calculation of the last quantity, by performing a gauge transformation for each point in space, leads to gauge-invariant values of the shielding tensors.

Both CSGT and GIAO methodologies are very useful, although it seems that the GIAO procedure is somewhat superior, especially with respect to the convergence of the calculated properties upon extension of the basis set used.^{9,19–23} Other methods, such as IGLO^{24,25} (Individual Gauge for Localized Orbitals) and LORG^{26,27} (localized orbital/local origin), seem to be less preferable at the present state of this subject, taking into account the computational cost and the effectiveness of calculation of the GIAO and CSGT methods.

It is beyond doubt that studies of various methods for achievement of gauge invariance, especially with respect to inclusion of the dynamic electron correlation effects²⁸ and to the basis set size,⁹ are of substantial methodological importance. (Let us briefly recall at this point that the correlation energy arising from overestimation of short-range electron-electron repulsion is usually denoted as a »dynamic« correlation, in contrast to the part arising from long-range correlation (*e.g.* observable in molecular dissociation), which is referred to as »non-dynamic« (or static). Thus, it is important to clarify that the term »dynamic« is not used within this paper in the same way as in the context of time-dependent methods). A number of studies have been published on the subject of achievement of gauge invariance^{19,29–37} but a definite conclusion on the choice of optimal computational methodology does not seem to have been reached. The last statement especially holds for the ability of density functional theory-based (DFT) methods to predict accurately the second order magnetic response properties. Since the DFT approach is computationally far less demanding than the wavefunction-based methodologies that explicitly include the dynamic electron correlation effects, it is of great importance to establish a density-based method for a chemically reasonable prediction of NMR chemical shift tensors. Although the Hohenberg-Kohn theorem³⁸ establishes a one-to-one correspondence between the »external (with respect to electronic subsystem) potential« and the corresponding density, implying that the electronic energy of a given molecular system is a definite functional of the corresponding density,^{38–40} it does not give the exact form of this functional. It is important to note at this point that the foregoing statement is the main cause of in a sense, the semi-empirical character of DFT approaches. Various types of exchange and correlation functionals have been proposed^{41–47} either on a more mathematical or physical basis, but almost all of the proposed functionals were constructed primarily having the energetics of molecular systems in mind. Although some of them (mainly the gradient corrected ones) have been shown to be remarkably accurate in prediction of other molecular properties, such as harmonic force constants,^{48–50} it is still of certain interest to test their performances for prediction of the second order magnetic response properties. Several systematic studies have already been devoted to this sub-

ject,^{19,36–39} but mainly with respect to the correlation between the computed isotropic shieldings and the measured chemical shifts. It seems that little attention has been paid to the question of performances of various theoretical approaches regarding the prediction of the relative shielding values with respect to a given center within the same molecule and the substituent effects.

Continuing our research on the choice of the optimal computational methodology that would be able to reproduce the chemical shift values with chemical accuracy, in the present paper, we report a HF SCF and density functional study of isotropic ¹³C and ¹H chemical shifts for 2-adamantanone, a system characterized by a highly stiffened structure. Due mainly to their rigid and thus well-defined frameworks, adamantane and related systems are almost ideal model systems for a study of both the ¹³C chemical shifts and substituent effects on these quantities. For the purpose of the present study, we have used the optimized geometries of 2-adamantanone at two gradient corrected density functional levels of theory^{39,40} with a DZP quality basis set for both the system of interest and the standard for calculation of isotropic chemical shifts (TMS). The performances of various density functional methodologies and the conventional HF SCF procedure in predicting both the ¹³C and ¹H isotropic chemical shifts and the substituent effects (with respect to adamantane as parent compound) were tested, along with the efficiency of GIAO, CSGT and IGAIM algorithms for achieving gauge independence.

EXPERIMENTAL

NMR Measurements

The NMR data of adamantane and 2-adamantanone are available in literature.⁵¹ However, we have remeasured the ¹H and ¹³C NMR spectra of these compounds in higher magnetic fields, attaining greater precision.⁵² The spectra were recorded with a Varian Gemini 300 spectrometer, operating at 75.46 MHz for the ¹³C nucleus. The samples were dissolved in CDCl₃ and measured at 20 °C in 5 mm NMR tubes. Concentrations of samples were 0.1 mol dm⁻³ for ¹H and 0.2 mol dm⁻³ for ¹³C measurements. Chemical shifts (ppm) were referred to TMS as internal standard. Digital resolution was 0.3 Hz per point in ¹H and 0.5 Hz per point in ¹³C NMR one-dimensional spectra. The techniques used were: standard ¹H, ¹³C broadband proton decoupling, ¹³C gated decoupling, COSY and HETCOR. The Waltz-16 modulation was used for proton decoupling. The COSY spectra were recorded in the magnitude mode with 1024 points in F2 dimension and 256 increments in F1 dimension, zero-filled to 1024 points. Increments were measured with 16 scans, 4500 Hz spectral width and a relaxation delay of 1 s. The corresponding digital resolution was 8.9 Hz per point and 17.6 Hz per point in F2 and F1 dimensions, respectively. The HETCOR spectra were recorded with 2048 points in F2 dimension and 256 increments in F1 dimension. The latter was zero-filled to 512

points. Increments were recorded with 64 scans with a relaxation delay of 0.8 s. Spectral widths were 19000 Hz in F2 and 4500 Hz in F1 dimensions, giving digital resolution of 18.6 Hz per point and 17.6 Hz per point, respectively.

COMPUTATIONAL DETAILS

The geometries of 2-adamantanone and tetramethylsilane (TMS) were fully optimized in redundant internal coordinates with Schlegel's gradient optimization algorithm⁵³ (calculating the energy derivatives with respect to nuclear coordinates analytically). Geometry optimizations were performed at two gradient-corrected density functional levels of theory. Within the first, a combination of Becke's exchange functional⁴² with the Lee-Yang-Parr correlation one⁴⁴ (the methodology denoted as BLYP) was used, while in the second, a combination of Becke's three-parameter adiabatic connection exchange functional (B3)⁴⁷ with LYP (B3LYP) was employed. Standard 6-31G(d,p) basis set of DZP quality was used for orbital expansion in solving the Kohn-Sham equations.⁴¹ The Kohn-Sham equations were solved iteratively for the gradient-corrected functionals (instead of performing a single integration after local spin density iterations). The stationary points found on the molecular potential energy hypersurfaces were characterized by numerical harmonic vibrational analyses. The absence of imaginary frequencies (negative eigenvalues of the Hessian matrices) confirmed that the stationary points correspond to real minima, instead of being saddle points. Complete harmonic vibrational analyses of the mentioned species will be published elsewhere.

Calculations of Isotropic Chemical Shifts

The ¹H and ¹³C NMR shielding tensors for the BLYP/6-31G(d,p) and B3LYP/6-31G(d,p) optimized geometries of the mentioned species were calculated using three previously discussed methodologies for achievement of gauge independence: the Gauge Independent Atomic Orbitals (GIAO) method, Continuous Set of Gauge Transformations (CSGT) methodology and the Individual Gauge for Atoms In Molecules (IGAIM) approach (for a more thorough description of these methods, see our previous paper).¹⁵ These calculations were performed at the HF, BLYP and B3LYP levels of theory, using a TZP quality basis set 6-311G(d,p) for orbital expansion, as well as at the MPW1PW91/6-311+G(2d,p) level. The latter approach has been recently proposed and is based on a combination of the exchange Perdew-Wang 1991 functional, as modified by Adamo and Barone,⁵⁴ with the Perdew and Wang's 1991 gradient-corrected correlation functional.⁵⁵ The 6-311+G(2d,p) basis set includes a set of diffuse sp functions on all carbons and oxygen, as well as two sets of d functions on these atoms. In all density functional calculations, the fine (75, 302) grid was used for numerical integration (75 radial and 302 angular integration points).^{39,40} Note that while the BLYP methodology is non-hybrid (it includes no HF exchange), the B3LYP and the MPW1PW91 ones contain an admixture of HF exchange (*i.e.* they are of hybrid form).

The isotropic shielding values, defined as:

$$\sigma_{\text{iso}} = \frac{1}{3}(\sigma_{11} + \sigma_{22} + \sigma_{33}) \quad (2)$$

(σ_{ii} being the principal tensor components) were used to calculate the isotropic chemical shifts δ with respect to TMS ($\delta_{\text{iso}}^{\text{X}} = \sigma_{\text{iso}}^{\text{TMS}} - \sigma_{\text{iso}}^{\text{X}}$).

It is worth noting at this point that the BLYP and B3LYP combinations of exchange and correlation functionals used in the present work for calculation of magnetic shielding properties do not include the magnetic field dependence explicitly.³⁵ However, they have been shown to yield rather accurate predictions of some other molecular properties.^{35,48} On the other hand, the MPW1PW91 combination of functionals was specifically designed to overcome the poor behavior of other widely used functionals in the low-density and large-gradient regions.⁵⁴

As mentioned before, within the GIAO methodology, for calculation of magnetic properties, explicitly field-dependent wavefunctions are used, of the following form:

$$\chi_{\mu}(\vec{B}) = \exp\left[-\frac{i}{2c}(\vec{B} \times \vec{R}_{\mu}) \cdot \vec{r}\right] \cdot \chi_{\mu}(\vec{0}) \quad (3)$$

(χ_{μ} being the field-dependent basis function, \vec{R}_{μ} the position vector, $\chi_{\mu}(\vec{0})$ denotes the (usual) field-independent function, while c is the speed of light in vacuum and $i = \sqrt{-1}$). On the other hand, the CSGT approach is based on the expression for the shielding tensor components for nucleus X in terms of the induced first-order electronic current density $\mathcal{J}^{(1)}(r)$:

$$\sigma_{\text{X}}^{\alpha\beta} = \frac{\partial^2 E}{\partial B^{\alpha} \partial m_{\text{X}}^{\beta}} = -\frac{1}{Bc} \int [\vec{r}_{\text{X}} \times \mathcal{J}_{\alpha}^{(1)}(r) / r_{\text{X}}^3]_{\beta} d\vec{r}_{\text{X}} \quad (4)$$

Within this method, the gauge-invariance is achieved by accurate calculation of the induced first order electronic current density, performing a gauge transformation for each point in space.

All calculations were carried out with the Gaussian 98 series of programs.⁵⁶

RESULTS AND DISCUSSION

Optimized geometry parameters for 2-adamantanone calculated at the BLYP/6-31G(d,p) and B3LYP/6-31G(d,p) levels of theory are given in Table I, together with the experimental data (for more detailed comments, see Ref. 57). The molecular structure and atomic numbering scheme are shown in Figure 1. As can be seen, the agreement between theory and experiment is very good. It has been long recognized that accurate predictions of molecular geometries are of essential importance for reliable calculations of magnetic properties. Although it is sometimes convenient even to use the available experimental geometry, in order to have consistent results with the other systems previously studied by us,¹⁵ as well as to be able to compare the present results and calculate the substituent effects with respect to adamantane as parent compound, we relied on the DFT optimized geometries. Since the agreement with the available experimental data is fairly good, and further,

TABLE I

Theoretical and experimental⁵⁷ geometry parameters for 2-adamantanone (all distances in nm, all angles in degrees) optimized by BLYP/6-31G(d,p) and B3LYP/6-31G(d,p)

Parameter	BLYP	B3LYP	Exp.
$r(\text{C}=\text{O})$	0.1229	0.1217	0.1240
$r(\text{C1-C2})$	0.1540	0.1527	0.1540
$\alpha(\text{C2C1C2})$	112.4	112.6	109.5
$\alpha(\text{C1C2C3})$	108.4	108.3	109.5
$\alpha(\text{C2C3C4})$	109.8	109.8	109.5
$\alpha(\text{C1C2H})$	108.4	108.3	109.5
$\alpha(\text{OC1C2})$	123.8	123.7	–

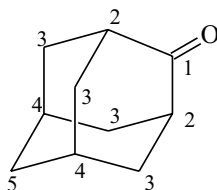


Figure 1. Structure and atomic numbering of 2-adamantanone.

the derivatives of the form $(\partial\sigma/\partial q_i)$ (q_i being a geometry parameter) are often rather small for both ^{13}C and ^1H shieldings,⁵⁸ we regard the adopted approach to be fully appropriate.

The computed isotropic ^{13}C chemical shifts (with respect to TMS) for 2-adamantanone at both HF/6-311G(d,p) as well as at density functional BLYP/6-311G(d,p), B3LYP/6-311G(d,p) and MPW1PW91/6-311+G(2d,p) levels of theory (employing both GIAO and CSGT methods for achievement of gauge independence) are presented in Tables II and III. The IGAIM values at the corresponding levels of theory yield essentially the same results as CSGT (which differ by an order of magnitude of 10^{-2} – 10^{-3}) and only the latter are presented. In Tables IV and V, the relative shift values with respect to the most deshielded center (carbonyl C) are given. The substituent effects with respect to adamantane as parent compound, expressed as differences in the isotropic shielding values are presented in Table VI. In order to be able to obtain the substituent effect with respect to adamantane as parent compound at the MPW1PW91/6-311+G(2d,p) level, we have calculated the MPW1PW91/6-311+G(2d,p) magnetic shielding tensors for the BLYP/6-31G(d,p) optimized

TABLE II

Theoretical isotropic ^{13}C chemical shifts computed with respect to TMS for the BLYP/6-31G(d,p) optimized geometry of 2-adamantanone and experimental isotropic chemical shift values. HF, BLYP and B3LYP calculations were performed with the 6-311G(d,p), while the MPW1PW91 ones with the 6-311+G(2d,p) basis set.

	HF	BLYP	B3LYP	MPW1PW91	Experimental
CSGT					
C1	215.8	214.2	216.7	221.2	218.5
C2	42.6	56.5	53.4	48.2	46.7
C3	34.5	46.7	43.8	38.6	39.0
C4	28.0	39.6	36.8	29.7	27.1
C5	34.0	43.7	41.4	35.9	36.0
GIAO					
C1	221.3	220.4	222.6	221.4	218.5
C2	44.7	58.4	55.2	48.4	46.7
C3	36.2	48.0	45.1	38.6	39.0
C4	28.2	39.1	36.3	29.7	27.1
C5	35.4	44.8	42.5	35.8	36.0

TABLE III

Theoretical isotropic ^{13}C chemical shift values computed with respect to TMS for the B3LYP/6-31G(d,p) optimized geometry of 2-adamantanone and experimental isotropic chemical shift values. HF, BLYP and B3LYP calculations were performed with the 6-311G(d,p), while the MPW1PW91 ones with the 6-311+G(2d,p) basis set.

	HF	BLYP	B3LYP	MPW1PW91	Experimental
CSGT					
C1	212.8	212.2	214.4	218.9	218.5
C2	41.8	55.5	52.4	47.3	46.7
C3	34.4	46.5	43.6	38.4	39.0
C4	27.2	38.7	35.9	28.9	27.1
C5	33.9	43.6	41.3	35.8	36.0
GIAO					
C1	218.0	218.2	220.1	219.0	218.5
C2	43.8	57.4	54.2	47.5	46.7
C3	35.9	47.7	44.8	38.3	39.0
C4	27.4	38.1	35.4	28.9	27.1
C5	35.2	44.6	42.3	35.6	36.0

TABLE IV

Theoretical isotropic ^{13}C chemical shift values computed with respect to the most deshielded internal center (carbonyl C) for the BLYP/6-31G(d,p) optimized geometry of 2-adamantanone and the corresponding differences of experimental isotropic chemical shift values. HF, BLYP and B3LYP calculations were performed with the 6-311G(d,p), while the MPW1PW91 ones with the 6-311+G(2d,p) basis set.

	HF	BLYP	B3LYP	MPW1PW91	Experimental
CSGT					
C1	0.0	0.0	0.0	0.0	0.0
C2	173.2	157.7	163.3	173.0	171.8
C3	181.3	167.4	172.8	182.6	179.5
C4	187.8	174.6	179.9	191.4	191.4
C5	181.9	170.5	175.2	185.3	182.5
GIAO					
C1	0.0	0.0	0.0	0.0	0.0
C2	176.6	162.0	167.3	173.0	171.8
C3	185.1	172.4	177.4	182.8	179.5
C4	193.1	181.3	186.2	191.7	191.4
C5	185.9	175.6	180.1	185.6	182.5

TABLE V

Theoretical isotropic ^{13}C chemical shift values computed with respect to the most deshielded internal center (carbonyl C) for the B3LYP/6-31G(d,p) optimized geometry of 2-adamantanone and the corresponding differences of experimental isotropic chemical shift values. HF, BLYP and B3LYP calculations were performed with the 6-311G(d,p), while the MPW1PW91 ones with the 6-311+G(2d,p) basis set.

	HF	BLYP	B3LYP	MPW1PW91	Experimental
CSGT					
C1	0.0	0.0	0.0	0.0	0.0
C2	171.0	156.7	162.0	171.6	171.8
C3	178.4	165.7	170.8	180.5	179.5
C4	185.5	173.5	178.5	190.0	191.4
C5	178.9	168.6	173.1	183.1	182.5
GIAO					
C1	0.0	0.0	0.0	0.0	0.0
C2	174.2	160.8	165.9	171.5	171.8
C3	182.1	170.5	175.3	180.7	179.5
C4	190.7	180.1	184.7	190.1	191.4
C5	182.8	173.6	177.8	183.4	182.5

TABLE VI

Theoretical substituent effects on the isotropic ^{13}C chemical shift values computed with respect to adamantane as parent compound for the BLYP/6-31G(d,p) optimized geometries of 2-adamantanone and experimental substituent effects on isotropic chemical shifts. HF, BLYP and B3LYP calculations were performed with the 6-311G(d,p), while the MPW1PW91 ones with the 6-311+G(2d,p) basis set.

	HF	BLYP	B3LYP	MPW1PW91	Experimental
CSGT					
C1	181.3	169.4	174.2	184.4	180.9
C2	15.0	16.1	16.6	17.7	18.5
C3	0.0	1.9	1.3	1.8	1.4
C4	0.4	-0.8	0.0	-0.8	-1.1
C5	-0.5	-1.1	-1.1	-0.9	-1.6
GIAO					
C1	187.7	175.7	181.0	184.7	180.9
C2	17.9	19.6	20.4	17.9	18.5
C3	2.6	3.3	3.5	1.9	1.4
C4	1.4	0.3	1.5	-0.8	-1.1
C5	1.8	0.1	0.9	-0.9	-1.6

TABLE VII

Theoretical and experimental ^{13}C and ^1H isotropic chemical shifts, all values in ppm with respect to TMS, for adamantane. Calculations were performed at the MPW1PW91/6-311+G(2d,p)//BLYP/6-31G(d,p) level of theory.

	C(t)^{a}		C(s)^{a}	
	CSGT	GIAO	CSGT	GIAO
MPW1PW91	30.5	30.5	36.8	36.7
Experimental	28.2		37.6	
	H(t)^{a}		H(s)^{a}	
	CSGT	GIAO	CSGT	GIAO
MPW1PW91	1.6	1.8	1.7	1.7
Experimental	1.9		1.8	

^a »s« and »t« denote, respectively, a secondary and tertiary carbon or hydrogen atom.

geometry for adamantane, which was reported in our previous paper.¹⁵ The theoretical results and experimental results obtained here are collected in Table VII. The following conclusions can be straightforwardly derived on the basis of the data presented in Tables II–VII.

First of all, on an absolute scale, the isotropic ^{13}C chemical shift values (computed with respect to TMS) at the HF/6-311G(d,p) level are significantly superior to the BLYP and B3LYP/6-311G(d,p) ones, the last two methodologies leading to somewhat too deshielded centers. Such conclusions are valid regardless of the method for achievement of gauge invariance. On the other hand, the MPW1PW91/6-311+G(2d,p) values are in excellent agreement with the experimental data, the CSGT approach showing a very slight superiority over GIAO. Obviously, the computed isotropic chemical shifts for the B3LYP/6-311G(d,p) optimized geometry are superior to those for the BLYP/6-311G(d,p) one. The weak performances of the »standard« gradient-corrected DFT approaches based on the BLYP and B3LYP combinations of functionals in reproducing the experimental isotropic chemical shifts was already discussed in our previous paper. Namely, as mentioned before, these functionals have been parametrized for calculation of energetic properties, and are thus expected to perform best for calculations of such properties.^{35,39,40} Due to the underestimation of the $\varepsilon_a - \varepsilon_i$ energy differences (where subscript a refers to virtual orbitals, while i refers to occupied ones), the DFT methods overestimate the paramagnetic shielding terms, leading exactly to »too deshielded« centers. The paramagnetic contribution³⁵ to the shielding tensor component within the DFT GGA approximation is given by:

$$\sigma_{\text{p}}^{\text{X}\alpha\beta} = -\sum_{j=1}^n \sum_{b=n+1}^m \frac{\langle b|l^\alpha|j\rangle\langle j|l_{\text{X}}^\beta r_{\text{X}}^{-3}|b\rangle + \langle b|l_{\text{X}}^\alpha r_{\text{X}}^{-3}|j\rangle\langle j|l^\beta|b\rangle}{(\varepsilon_b - \varepsilon_j)} \quad (5)$$

(r_{X} being the distance of electron from nucleus X, l the angular momentum operator, while the Greek superscripts denote vector or tensor components). From the physical viewpoint, the underestimation of the $\varepsilon_a - \varepsilon_i$ terms is a consequence of the fact that the BLYP and B3LYP functionals vanish too quickly to zero, which leads to wrong Kohn-Sham solutions for the virtual states. Any perturbation theoretic approach based on these solutions would therefore lead to erroneous predictions. An attempt to overcome this weak point of the GGA approximation was recently presented, based on the usage of two novel functionals – HCTH and its asymptotically corrected variant – HCTH(AC).³⁵ Another efficient algorithm for improvement of these results is based on Malkin’s sum-over-states density functional perturbation theory (SOS-DFPT).³⁵ It is worth noting that the last approach leads to a substantial improvement in the calculated magnetic properties.

The same conclusions as for the isotropic chemical shifts are valid also for the relative shift values computed with respect to the most deshielded center within the molecule – carbonyl C. The HF/6-311G(d,p) values are superior to the BLYP and B3LYP/6-311G(d,p) ones, while the MPW1PW91/6-

311+G(2d,p) ones agree excellently with the experimental data. It is worth mentioning, however, that despite the inferior performances of the BLYP and B3LYP methodologies in computation of the isotropic chemical shifts, the computed values correlate excellently with the experimental data. Although the number of data is rather small in the present case, thus preventing generalization of the previous statement, the range of δ values spanned is rather large, and the excellent linear correlations ($r^2 > 0.999$) may not be regarded as purely fortuitous. In Figure 2, the B3LYP/6-311G(d,p)//B3LYP/6-31G(d,p) isotropic chemical shift values are plotted *vs.* the experimental data. This linear correlation found for all of the GGA DFT levels of theory employed in the present study is a further proof that much of the error in the ^{13}C magnetic shielding calculations is systematic in nature.¹⁹

Regarding the substituent effects on the ^{13}C isotropic chemical shifts (with respect to adamantane as parent compound), the situation seems to be reversed. Except for the most deshielded center (carbonyl C), for all other carbon atoms the DFT results are significantly superior to the HF SCF ones. The MPW1PW91 combination of functionals is again significantly superior to the other DFT approaches. It is interesting to note that even for the relative shift values, within the most deshielded intramolecular carbon center, if carbonyl C is excluded, the DFT results are superior to the HF SCF. However, since due to the high symmetry of 2-adamantanone (C_{2v}) the

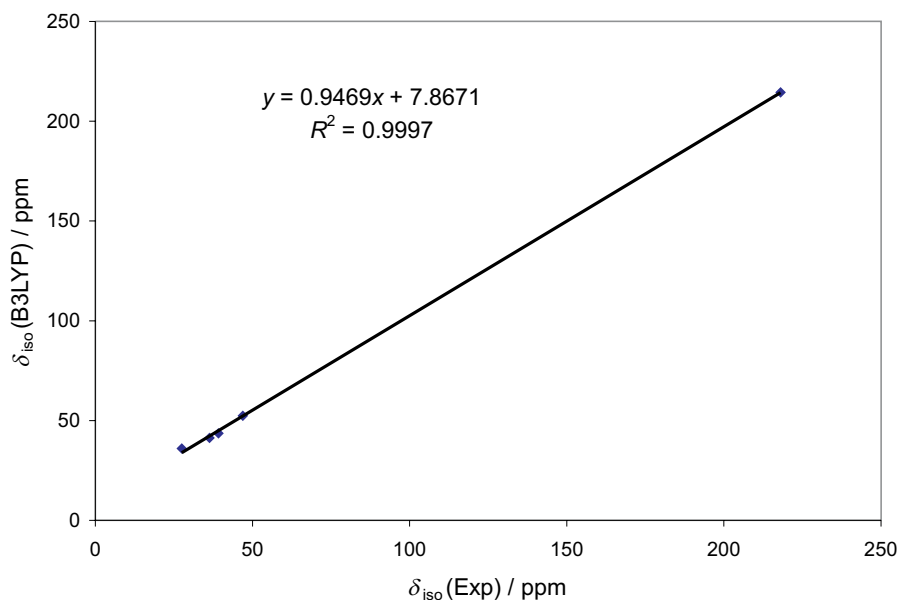


Figure 2. Plot of the B3LYP/6-3116(d,p) computed isotropic ^{13}C chemical shifts *vs.* experimental ^{13}C chemical shifts.

number of symmetry inequivalent carbon atoms is rather small, it is impossible to generalize such a statement, as it was possible for [3.1.1] propellane. All these findings, however, imply that the DFT methods based on »standard« (energy-optimized) functionals, although leading to poorer absolute agreement with the experimental data, perform better in the sense that the error is more systematical in nature. That is the main reason why the substituent effects are better reproduced by the DFT than HF methods. A possible explanation for this »systematic« nature of errors in the GGA DFT calculations of magnetic shielding tensors is a rather constant underestimation of the $\varepsilon_a - \varepsilon_i$ energy differences for different, yet chemically similar systems. However, more theoretical work would be needed to prove such an assumption. Inclusion of a combination of functionals (MPW1PW91), which has been parameterized specifically to overcome the poor long-range behavior of other GGA functionals, leads to a far better description of virtual electronic states, thus allowing for a much more reliable values of the paramagnetic part of the shielding tensors.

Isotropic ^1H chemical shift values (computed with respect to TMS) for the BLYP/6-31G(d,p) and B3LYP/6-31G(d,p) optimized geometries of 2-adamantanone are presented in Tables VIII and IX, together with the available experimental data. As can be seen, the agreement of the MPW1PW91/6-311+G(2d,p) values with the experiment is excellent, and also far better than in the case of all other approaches.

TABLE VIII

Theoretical isotropic ^1H chemical shift values computed with respect to TMS for the BLYP/6-31G(d,p) optimized geometry of 2-adamantanone and experimental isotropic chemical shift values. HF, BLYP and B3LYP calculations were performed with the 6-311G(d,p), while the MPW1PW91 ones with the 6-311+G(2d,p) basis set.

	HF	BLYP	B3LYP	MPW1PW91	Experimental
CSGT					
H(C2)	1.6	1.8	1.7	2.2	2.5
H _{eq} (C3)	1.3	1.9	1.7	1.9	2.1
H _{ax} (C3)	1.2	1.8	1.7	1.8	2.0
H(C4)	1.2	1.6	1.5	1.7	1.9
H(C5)	1.4	1.8	1.7	1.8	2.0
GIAO					
H(C2)	2.3	2.3	2.3	2.4	2.5
H _{eq} (C3)	1.7	2.2	2.0	2.0	2.1
H _{ax} (C3)	1.6	2.1	2.0	1.9	2.0
H(C4)	1.6	1.9	1.9	1.8	1.9
H(C5)	1.6	2.0	1.9	1.9	2.0

TABLE IX

Theoretical isotropic ^1H chemical shift values computed with respect to TMS for the B3LYP/6-31G(d,p) optimized geometry of 2-adamantanone and experimental isotropic chemical shift values. HF, BLYP and B3LYP calculations were performed with the 6-311G(d,p), while the MPW1PW91 ones with the 6-311+G(2d,p) basis set.

	HF	BLYP	B3LYP	MPW1PW91	Experimental
CSGT					
H(C2)	1.5	1.7	1.7	2.1	2.5
H _{eq} (C3)	1.3	1.9	1.7	1.9	2.1
H _{ax} (C3)	1.3	1.8	1.7	1.8	2.0
H(C4)	1.2	1.6	1.5	1.7	1.9
H(C5)	1.4	1.9	1.7	1.8	2.0
GIAO					
H(C2)	2.2	2.3	2.3	2.4	2.5
H _{eq} (C3)	1.7	2.2	2.0	2.0	2.1
H _{ax} (C3)	1.6	2.1	2.0	1.9	2.0
H(C4)	1.6	1.9	1.9	1.8	1.9
H(C5)	1.7	2.1	2.0	1.9	2.0

CONCLUSIONS

The ^{13}C and ^1H isotropic chemical shift values (with respect to TMS), together with the substituent effects on the ^{13}C shieldings (with respect to adamantane), were calculated at the HF, BLYP and B3LYP/6-311G(d,p) as well as at MPW1PW91/6-311+G(2d,p) levels of theory for the BLYP and B3LYP/6-31G(d,p) optimized geometries of 2-adamantanone. For both studied properties, the MPW1PW91/6-311+G(2d,p) approach leads to an excellent agreement with the experimental NMR data. Although the HF SCF approach is superior to the BLYP and B3LYP ones in predicting the isotropic chemical shifts, the DFT methodologies predict the substituent effects much better than the HF one. The last finding, together with the better correlation of DFT isotropic shieldings with the experimental data, supports the assumption that much of the absolute error in predicting the isotropic chemical shifts at the DFT levels shows a rather systematic nature. The underestimation of the $\varepsilon_a - \varepsilon_i$ energy differences (where subscript a refers to virtual orbitals, while i refers to occupied ones) with the DFT methods, leading to an overestimation of the paramagnetic shielding terms, seems to be rather constant for different, but yet chemically similar species. Inclusion of a combination of functionals (MPW1PW91), parameterized specifically to overcome the poor long-range behavior of other GGA functionals, leads to much more reliable values of the paramagnetic part of the shielding tensors, and thus a far better overall agreement with the experimental data.

REFERENCES

1. G. A. Olah, T. Shamma, A. Burrichter, G. Rasul, and G. K. S. Prakash, *J. Am. Chem. Soc.* **119** (1997) 12923–12928.
2. K. B. Wiberg and N. McMurdie, *J. Am. Chem. Soc.* **116** (1994) 11990–11998.
3. J. F. Haw, J. B. Nicholas, T. Xu, L. W. Beck, and D. B. Ferguson, *Acc. Chem. Res.* **29** (1996) 259–267.
4. A. C. de Dios, J. G. Pearson, and E. Oldfield, *Science* **260** (1993) 1491–1496.
5. D. Sitkoff and D. A. Case, *J. Am. Chem. Soc.* **119** (1997) 12262–12273.
6. V. Copie, J. A. Battles, J. M. Schwab, and D. A. Torchia, *J. Biomol. NMR* **7** (1996) 335–340.
7. K. R. MacKenzie, J. H. Prestegard, and D. M. Engelman, *J. Biomol. NMR* **7** (1996) 256–260.
8. C. E. Dykstra, *Quantum Chemistry & Molecular Spectroscopy*, Prentice Hall, New Jersey, 1992, pp. 336–347.
9. J. R. Cheeseman, G. W. Trucks, T. A. Keith, and M. J. Frisch, *J. Chem. Phys.* **104** (1996) 5497–5509.
10. G. A. Webb, in: J. A. Tossell (Ed.), *Nuclear Magnetic Shieldings and Molecular Structure*, Kluwer Publishers, Netherlands, 1993, pp. 1–25.
11. R. Ditchfield, *Mol. Phys.* **27** (1974) 789–807.
12. F. London, *Phys. Radium* **8** (1937) 397–410.
13. K. Wolinski, J. F. Hinton, and P. Pulay, *J. Am. Chem. Soc.* **112** (1990) 8251–8260.
14. P. Pulay, J. F. Hinton, and K. Wolinski, in: J. A. Tossell (Ed.), *Nuclear Magnetic Shieldings and Molecular Structure*, Kluwer Publishers, Netherlands, 1993, pp. 243–262.
15. D. Vikić-Topić and Lj. Pejov, *Croat. Chem. Acta* **73** (2000) 1057–1075.
16. T. A. Keith and R. F. W. Bader, *Chem. Phys. Lett.* **194** (1992) 1–8.
17. T. A. Keith and R. F. W. Bader, *Chem. Phys. Lett.* **210** (1993) 223–231.
18. T. A. Keith and R. F. W. Bader, *J. Chem. Phys.* **99** (1993) 3669–3682.
19. P. R. Rablen, S. A. Pearlman, and J. Finkibiner, *J. Phys. Chem. A* **103** (1999) 7357–7363.
20. V. G. Malkin, O. L. Malkina, M. E. Casida, and D. R. Salahib, *J. Am. Chem. Soc.* **116** (1994) 5898–5908.
21. G. A. Olah, A. Burrichter, G. Rasul, K. O. Christe, and G. K. S. Prakash, *J. Am. Chem. Soc.* **119** (1997) 4345–4352.
22. J. F. Hinton, P. L. Guthrie, P. Pulay, K. Wolinski, and G. Fogarasi, *J. Magn. Reson.* **96** (1992) 154–158.
23. C. McMichael Rohlfing, L. C. Allen, and R. Ditchfield, *J. Chem. Phys.* **79** (1983) 4958–4966.
24. M. Schindler, *J. Am. Chem. Soc.* **109** (1987) 1020–1033.
25. W. Kutzelnigg, Ch. van Wullen, U. Fleischer, R. Franke, and T. v. Mourik, in: J. A. Tossell (Ed.), *Nuclear Magnetic Shieldings and Molecular Structure*, Kluwer Publishers, Netherlands, 1993, pp. 141–161.
26. A. E. Hansen and T. D. Bouman, in: J. A. Tossell (Ed.), *Nuclear Magnetic Shieldings and Molecular Structure*, Kluwer Publishers, Netherlands, 1993, pp. 117–140.
27. W. Kutzelnigg, *Isr. J. Chem.* **19** (1980) 193–200.
28. H. Fukui, T. Baba, H. Matsuda, and K. Miura, *J. Chem. Phys.* **100** (1994) 6608–6613.
29. J. A. Tossell, *Chem. Phys. Lett.* **303** (1999) 435–440.
30. P. Cmoch, J. W. Wiench, L. Stefaniak, and G. A. Webb, *Spectrochim. Acta* **55A** (1999) 2207–2214.

31. A. M. Orendt, J. C. Facelli, and D. M. Grant, *Chem. Phys. Lett.* **302** (1999) 499–504.
32. J. A. Kintop, W. V. M. Machado, M. Franco, and H. E. Toma, *Chem. Phys. Lett.* **309** (1999) 90–94.
33. V. Galasso, *Chem. Phys.* **241** (1999) 247–255.
34. M. Pecul and J. Sadlej, *Chem. Phys.* **234** (1998) 111–119.
35. P. J. Wilson, R. D. Amos, and N. C. Handy, *Mol. Phys.* **97** (1999) 757–768.
36. K. B. Wiberg, *J. Comp. Chem.* **20** (1999) 1299–1303.
37. M. Buhl, M. Kaupp, O. L. Malkina, and V. G. Malkin, *J. Comp. Chem.* **20** (1999) 91–105.
38. P. Hohenberg and W. Kohn, *Phys. Rev. B* **136** (1964) 864–871.
39. R. G. Parr and W. Yang, *Density Functional Theory of Atoms and Molecules*, Oxford University Press, Oxford, 1989.
40. J. M. Seminario, *An Introduction to Density Functional Theory in Chemistry*, in: J. M. Seminario and P. Politzer (Eds.), *Modern Density Functional Theory*, Elsevier Science B. V., Amsterdam, 1995, pp. 1–27.
41. W. Kohn and L. J. Sham, *Phys. Rev.* **140** (1965) 1133–1138.
42. A. D. Becke, *Phys. Rev. A* **38** (1988) 3098–3100.
43. S. H. Vosko, L. Wilk, and M. Nusair, *Can. J. Phys.* **58** (1980) 1200–1211.
44. C. Lee, W. Yang, and R. G. Parr, *Phys. Rev. B* **37** (1988) 785–789.
45. J. P. Perdew, *Phys. Rev. B* **33** (1986) 8822–8824.
46. J. P. Perdew and Y. Wang, *Phys. Rev. B* **45** (1992) 13244–13246.
47. A. D. Becke, *J. Chem. Phys.* **98** (1993) 5648–5652.
48. A. P. Scott and L. Radom, *J. Phys. Chem.* **100** (1996) 16502–16513.
49. Lj. Pejov, V. Stefov, and B. Šoptrajanov, *Vibr. Spectrosc.* **19** (1999) 435–439.
50. A. D. Esposti and F. Zerbetto, *J. Phys. Chem. A* **101** (1997) 7283–7291.
51. Z. Majerski, V. Vinković, and Z. Meić, *Org. Magn. Res.* **17** (1981) 169–171.
52. D. Vikić-Topić and Lj. Pejov, in: D. Vikić-Topić (Ed.), *Book of Abstracts of The 3rd International Dubrovnik NMR Course and Conference* (ISBN 953-6690-10-1), Zagreb, Croatia, 2000, p. 49.
53. H. B. Schlegel, *J. Comp. Chem.* **3** (1982) 214–218.
54. C. Adamo and V. Barone, *J. Chem. Phys.* **108** (1998) 664–675.
55. J. P. Perdew, J. A. Chevary, S. H. Vosko, K. A. Jackson, M. R. Pederson, D. J. Singh, and C. Fiolhais, *Phys. Rev. B* **46** (1992) 6671–6687.
56. M. J. Frisch, G. W. Trucks, H. B. Schlegel, G. E. Scuseria, M. A. Robb, J. R. Cheeseman, V. G. Zakrzewski, J. A. Montgomery, R. E. Stratmann, J. C. Burant, S. Dapprich, J. M. Millam, A. D. Daniels, K. N. Kudin, M. C. Strain, O. Farkas, J. Tomasi, V. Barone, M. Cossi, R. Cammi, B. Mennucci, C. Pomelli, C. Adamo, S. Clifford, J. Ochterski, G. A. Petersson, P. Y. Ayala, Q. Cui, K. Morokuma, D. K. Malick, A. D. Rabuck, K. Raghavachari, J. B. Foresman, J. Cioslowski, J. V. Ortiz, B. B. Stefanov, G. Liu, A. Liashenko, P. Piskorz, I. Komaromi, R. Gomperts, R. L. Martin, D. J. Fox, T. Keith, M. A. Al-Laham, C. Y. Peng, A. Nanayakkara, C. Gonzalez, M. Challacombe, P. M. W. Gill, B. G. Johnson, W. Chen, M. W. Wong, J. L. Andres, M. Head-Gordon, E. S. Replogle and J. A. Pople, *Gaussian 98* (Revision A.9), Gaussian, Inc., Pittsburgh PA, 1998.
57. C. E. Nordman and D. L. Schmitkons, *Acta Crystallogr. B* **18** (1965) 764–767.
58. A. K. Jameson and C. J. Jameson, *Chem. Phys. Lett.* **134** (1987) 461–466.

SAŽETAK**Proračuni kemijskih pomaka za geometrije optimizirane metodama DFT. Izotropni kemijski pomaci ^1H i ^{13}C i supstituentni efekti na zasjenjenje jezgri ^{13}C 2-adamantanona***Dražen Vikić-Topić i Ljupčo Pejov*

Vrijednosti izotropnih kemijskih pomaka ^1H i ^{13}C i supstituentnih efekata u odnosu na adamantan izračunane su uporabom algoritama CSGT, GIAO i IGAIM te baznih skupova HF, BLYP, B3LYP/6-311G(d, p) i MPW1PW91/6-311+G(2d, p) za optimizirane geometrije 2-adamantanona [BLYP/6-31G(d, p) i B3LYP/6-31G(d, p)], te su uspoređene s eksperimentalnim podacima.

Apsolutne vrijednosti izotropnih kemijskih pomaka, u odnosu na TMS, izračunane s baznim skupom MPW1PW91/6-311+G(2d, p) izvanredno se slažu s eksperimentalnim podacima. Nešto su slabije vrijednosti dobivene uporabom baznog skupa HF, no ipak bolje od onih dobivenih s baznim skupovima BLYP i B3LYP. Suprotno tome supstituentni efekti na zasjenjenja ^{13}C bolje se reproduciraju s baznim skupovima BLYP i B3LYP nego s baznim skupom HF. Vrijednosti supstituentnih efekata izračunane s baznim skupom MPW1PW91/6-311+G(2d, p) najbolje su od svih te daju izvanredno slaganje s eksperimentalnim rezultatima. Najvjerojatniji razlog tome je poništavanje pogrešaka zbog neodgovarajućeg opisa paramagnetnog doprinosa ukupnom tenzoru zasjenjenja u Kohn-Shamovu teorijskom pristupu te zbog sustavnih pogrešaka u teorijskom pristupu DFT.

Za sve bazne skupove vrijedi da izračunani izotropni kemijski pomaci jako dobro koreliraju s eksperimentalnim podacima pri čemu je slaganje s eksperimentom bitno bolje za bazne skupove DFT nego za bazni skup HF.